

INFLUENCE OF PIEZOELECTRIC ANISOTROPY ON ELECTROMECHANICAL PERFORMANCE OF ULTRASOUND NDT PROBES AT ELEVATED TEMPERATURES

UDC 620.179.16:681.586.7

Summary

When designing an ultrasound non-destructive (NDT) probe for high temperature applications, one has to take into account a multitude of temperature induced effects, such as the temperature dependence of key physical properties of probe materials. In this paper, the significant influence of temperature change on piezoelectric properties and piezoelectric anisotropy, and thus on the ultrasound properties of the whole probe, is discussed theoretically. This is demonstrated within the thermodynamic Landau-Ginzburg-Devonshire (LGD) framework and the KLM model of equivalent circuits for two different piezoelectric, acoustically active probe materials from the same family - barium titanate and lead titanate. These two materials are model materials for the whole family of piezoelectric perovskites, including the commercially widely used PZT and relaxor ferroelectrics PMN-PT and PZN-PT.

Key words: *non-destructive testing, ultrasound transducer, piezoelectric ceramic, piezoelectric anisotropy*

1. Introduction

A quasi-regular recurrence of disastrous accidents in nuclear power plants (NPPs) around the world (Three Mile Island loss of coolant and partial core meltdown in 1979, Chernobyl NPP steam explosion and meltdown in 1986, Mihama NPP steam explosion in 2004, Fukushima NPP cooling failure in 4 reactors followed by multiple meltdowns in 2011) has already been producing human losses, dreadful injuries, massive financial losses, electricity blackouts, and strong negative public opinion towards the utilization of nuclear energy for decades. Bearing in mind the lack of effective short term alternatives to nuclear power plants, the question of nuclear power plants safety hence remains crucial. Research and development of technologies for improving structural health control of such complex systems or its parts will continue to be of vital importance for many years to come. For a structural health inspection, each nuclear power plant has to follow rigorous standards, regulations and codes approved by national nuclear regulatory institutions. Accordingly, all such inspections have to be performed during plant outages. Since the inspections are performed during outages, the inspection techniques and technologies are adjusted to be effective at room temperature.

However, it turns out that if the condition of some power plant vital parts, such as a pipeline/steamline carrying saturated or superheated steam, is not monitored during operation,

in between outages, this may present a problem for an aging power plant. In situ condition monitoring techniques therefore should be developed to retain reliability and extend the lifetime of nuclear power plants. As a descriptive example of this problem, one can see the maintaining of the integrity of the above mentioned pipelines – high temperatures and pressures in pipelines and steamlines in nuclear power plants can lead to the formation of flaws and defects due to material degradation mechanisms such as corrosion, creep and fatigue over time. If undetected in advance, these critical features can cause catastrophic damage and failures which in turn could result in serious plant staff safety, environmental and financial consequences ([1], [2], [3]).

There has been an increased interest for research and development on diagnostic ultrasound transducers that are fully functional at elevated temperatures, [4]-[14]. At present, the main obstacle for effective design and building of such systems has been the poor functionality of their construction parts at elevated temperatures, especially of the acoustically active materials. Generally, there are several key issues discussed here: the acoustically active piezoelectric materials that generate ultrasound pulses upon electrical excitations, the passive acoustic materials (matching and backing layers), high temperature cables, high-temperature ultrasound transducers assembly and high temperature couplings, the most important transducer part being none the less the piezoelectric material, i.e., the temperature influence on its properties. When choosing a suitable piezoelectric material for a specific high temperature application, the ultrasound transducer designers are mostly led by the relation between the material Curie temperature (above which the piezoelectric properties are lost due to a phase transition to the paraelectric phase), T_C , and the needed operating temperature of the application. The principal and often the only rule taken into account, the “rule of thumb” is that the maximum operating temperature of the ultrasound transducer should not exceed $T_C/2$ of the piezoelectric crystal. It should be pointed out here that having this criterion is not enough - one has to be aware of many temperature induced effects in the piezoelectric materials. In this paper one of such effects – the piezoelectric anisotropy due to the presence and absence of multiple ferroelectric-ferroelectric phase transitions and its behaviour under material temperature changes is discussed. The most commonly used piezoelectric materials for ultrasound NDT applications are ferroelectric perovskites (such as piezoelectric ceramic $\text{Pb}(\text{Zn},\text{Ti})\text{O}_3$ – PZT). These materials are very interesting from both the application and the modelling point of view because they can go through sequences of phase transitions, both from a paraelectric phase to a ferroelectric phase at the Curie temperature and from ferroelectric to ferroelectric phase, which can be caused by temperature change [15], application of external bias fields [16], external mechanical stresses [17], and even changes of composition [18].

In this paper it is shown how temperature changes can influence the electromechanical and acoustical properties of an NDT transducer at different operating temperatures through the piezoelectric anisotropy of considered materials. The single crystal piezoelectric perovskite active materials are used as model examples: one that has several ferroelectric-ferroelectric phase transitions (barium titanate, BaTiO_3) and the other that has only one ferroelectric phase (lead titanate, PbTiO_3). We show how the presence of another ferroelectric phase in a perovskite piezoelectric seriously influences the performance of an ultrasound transducer performance if its temperature is changed. These effects will be modelled through the well-known, and widely accepted and experimentally verified, theoretical framework of the thermodynamic Landau-Ginzburg-Devonshire (LGD) phenomenology of electromechanical properties ([19], [20], [21]) by means of which we will predict the influence on ultrasound properties of a single normal beam NDT ultrasound probe, by using modelling in the KLM theory ([22], [23], [24]) and then conclude this discussion by generalising the results for the whole family of perovskite ferroelectrics.

2. LGD thermodynamic theory modelling

To discuss the temperature influence on the electromechanical (and finally ultrasound) response of an NDT probe that uses different single crystals as acoustically active materials (in our case barium titanate and lead titanate) we will first discuss the temperature behavior of the key piezoelectric coefficient in most ultrasound NDT applications – the longitudinal coefficient d_{33} , that quantifies the volume change when a piezoelectric material is subjected to an electric field, or the dielectric polarization change on the application of a stress, in which the direction of the change and of the applied fields are parallel. For this discussion we employ the thermodynamic Landau-Ginzburg-Devonshire phenomenological theory ([20], [21], [25]). We have calculated and discussed the orientation dependence of the longitudinal piezoelectric coefficient d_{33}^* in a general spatial direction, at room temperature the ferroelectric phases of BaTiO₃ and PbTiO₃ crystals (both tetragonal at room temperature), as well as a function of increasing temperature, and thus demonstrate the influence of the temperature and phase transitions presence and absence on the anisotropy of d_{33}^* . Barium titanate is an excellent model material for this problem. Upon cooling, it transforms from the cubic paraelectric phase (point group $m3m$) into the ferroelectric tetragonal phase (point group $4mm$) at 393 K, to the ferroelectric orthorhombic phase (point group $mm2$) at 278 K and to the ferroelectric rhombohedral phase (point group $3m$) at 183 K, [26].

The paraelectric phase of an intrinsically ferroelectric material is the one in which the spontaneous dielectric polarization does not exist ($P_{spontaneous} = 0$) – in that phase the ferroelectric behaves as any other dielectric material. This is usually the high temperature phase, and the phase transition point from a paraelectric to ferroelectric phase is called the Curie temperature (T_C). In such materials as barium titanate the phase transitions from paraelectric phase to a ferroelectric one, or even from one ferroelectric phase to another (barium titanate is such a material) can happen under the influence of external conditions: temperature change, application of external bias fields, mechanical stresses, or even by the change of the material composition, i.e. its chemical potential, which is a case for commercially widely used ferroelectric PZT. Barium titanate, the model material in this study, has a temperature driven series of phase transitions, which is caused by the translation of ions in the crystal lattice due to the creation and annihilation of corresponding phonon modes – an effect highly dependent on temperature, ([27], [28]).

Considering that the orthorhombic point group $mm2$ can be described as a special case of the monoclinic point group m [26], this sequence is similar to that observed in complex perovskite solid solutions PZT, that is widely commercially used, and PMN-PT and PZN-PT, promising ferroelectric relaxors with very strong piezoelectric response capabilities ([29], [30], [31]). BaTiO₃ is therefore a rich source for the determination and discussion of the phase transition effects on the orientation dependence of the piezoelectric coefficients in perovskite materials. On the other hand, PbTiO₃ exhibits only one, a tetragonal ferroelectric phase ([32], [33]) and is a good example of a material where the ferroelectric–ferroelectric phase transitions do not affect the temperature dependence of the piezoelectric properties. To calculate the temperature dependence of d_{33}^* , it is necessary to know the full set of the piezoelectric coefficients measured along the principal crystal axis for each crystal phase. The experimental values of these piezoelectric coefficients are not available for BaTiO₃ and PbTiO₃ (or any other perovskite) crystals over a sufficiently large temperature range.

In this paper, these piezoelectric coefficients are thus determined in the framework of the previously mentioned phenomenological LGD theory ([19], [20], [21]), that in fact studies the Taylor series expansion of the thermodynamic potential Gibbs free energy and its temperature change (for the description of the electromechanical properties of perovskites discussed in this paper, the series expansion up to the 6th order is sufficient):

$$\begin{aligned}
\Delta G &= \alpha_1(P_1^2 + P_2^2 + P_3^2) + \alpha_{11}(P_1^4 + P_2^4 + P_3^4) + \alpha_{111}(P_1^6 + P_2^6 + P_3^6) + \\
&+ \alpha_{12}(P_1^2 P_2^2 + P_1^2 P_3^2 + P_2^2 P_3^2) + \alpha_{112}(P_1^2(P_2^2 + P_3^2) + P_2^2(P_3^2 + P_1^2) + P_3^2(P_1^2 + P_2^2)) \\
&+ \alpha_{123}P_1^2 P_2^2 P_3^2 + \text{higher order terms} = \\
&= \{\text{for the tetragonal phase}\} = \\
&= \alpha_1 P_3^2 + \alpha_{11} P_3^4 + \alpha_{111} P_3^6 + \text{higher order terms} \tag{1}
\end{aligned}$$

Gibbs free energy is a thermodynamic potential useful for the description of phase transitions. It is defined as $G(p, T) = U + p \cdot V - T \cdot S$, where U is the internal energy, p is the pressure, V is the volume, T is the temperature, while S is the entropy of a discussed thermodynamic system. The change of the system Gibbs free energy, while changing its parameters, will show if a phase transition is feasible or not. The Landau-Ginzburg-Devonshire theory uses a Taylor series expansion of the Gibbs free energy in parameters that describe the discussed phases – in the case of ferroelectrics such as barium titanate, the phase parameter is the material spontaneous polarization (its direction and amplitude), [34].

The needed ferroelectric properties of BaTiO₃ and PbTiO₃, including the coefficients of the LGD function ($\alpha_1, \alpha_{11}, \alpha_{111}, \alpha_{12}, \dots$), are well documented in the literature. For the present calculations, we will take the LGD coefficients from Ref. [35] for BaTiO₃ and from Ref. [32] for PbTiO₃. The phenomenological calculations are done only for the tetragonal phase of both model materials, because they are both tetragonal at room temperature. The orientation dependence of the longitudinal piezoelectric coefficient in a general direction, d_{33}^* , is expressed in terms of the Euler angles (φ, θ, ψ) that are defined in the standard way [36]. The dielectric susceptibility, polarization, and piezoelectric coefficients in the crystallographic coordinate system of the tetragonal phase are denoted by η_{ij}^t , P_i^t and d_{ij}^t , respectively. The electrostrictive coefficients are denoted by Q_{ij} . The dielectric permittivity, ε_{ij} , is related to the dielectric susceptibility by the relation $\varepsilon_{ij} = \eta_{ij} + 1 \approx \eta_{ij}$. From the Gibbs free energy expression within the LGD theory, one can calculate the expressions for values of the spontaneous polarization and non-zero longitudinal, transversal and shear piezoelectric coefficients along the tetragonal phase crystal axes:

$$P_3^t = \sqrt{-\frac{\alpha_{11}}{3\alpha_{111}} + \frac{\sqrt{\alpha_{11}^2 - 3\alpha_1\alpha_{111}}}{3\alpha_{111}}}, \tag{2}$$

$$d_{15}^t = \varepsilon_0 \eta_{11}^t Q_{44} P_3^t, \tag{3}$$

$$d_{31}^t = 2\varepsilon_0 \eta_{33}^t Q_{12} P_3^t, \tag{4}$$

$$d_{33}^t = 2\varepsilon_0 \eta_{33}^t Q_{44} P_3^t. \tag{5}$$

For the tetragonal phase, the value of the longitudinal piezoelectric coefficient d_{33}^* in the crystallographic coordinate system along an arbitrary direction can be expressed as, [15] and [37]:

$$d_{33}^*(\theta) = \cos\theta(d_{15}^t \sin^2\theta + d_{31}^t \sin^2\theta + d_{33}^t \cos^2\theta) \tag{6}$$

where the angle θ describes a rotation away from the $[001]_t$ axis of the tetragonal cell [38], which is the axis along which the spontaneous polarization, P_3^t , is directed. It is important to mention here that the different qualitative temperature dependence of the shear coefficient d_{15}^t is directly related to the presence of the tetragonal–orthorhombic phase transition in BaTiO₃ and its absence in PbTiO₃ – this coefficient influences directly the overall qualitative behavior of the d_{33}^* coefficient. In the tetragonal ferroelectric phase of both materials studied in this paper, the shear piezoelectric coefficient d_{15}^t is proportional to the

dielectric susceptibility η_{11}^t along the $[100]_c$ axis (i.e., along the direction perpendicular to the direction of the spontaneous polarization P_3^t), ([20], [21], [32], [39]).

The qualitatively different orientation dependence of the d_{33}^{t*} for tetragonal BaTiO₃ and PbTiO₃ at room temperature and at elevated temperatures is modelled and presented in Fig. 1 and Fig. 2, while some numerical results extracted from these graphs are given in Table 1 and Table 2.

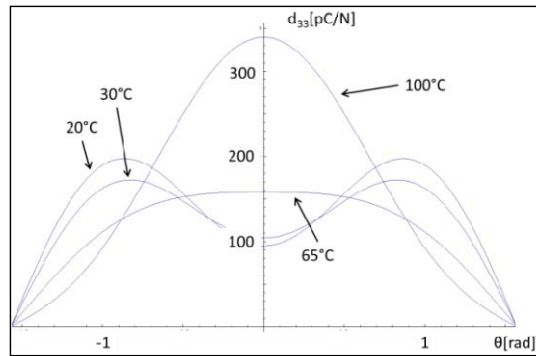


Fig. 1 Angular dependence of the longitudinal piezoelectric coefficient d_{33}^{t*} of tetragonal barium titanate for different temperatures. The angle θ represents the rotation direction away from the tetragonal polar axis. One can see that the maximum piezoelectric response direction in the tetragonal BaTiO₃ single crystal significantly and qualitatively changes with temperature.

Table 1 Maximum piezoelectric response of the tetragonal barium titanate with its corresponding directions at selected temperatures, compared with the values for the axial direction.

$T(^{\circ}\text{C})$	$d_{33max}(\text{pC/N})$	$\theta_{max}(^{\circ})$	$d_{33}(\theta=0^{\circ})$
20	198	49.5	95
30	172	47.3	104
65	158	0	158
100	340	0	340

One can see, for the tetragonal barium titanate (Fig. 1 and Table 1), that the maximal piezoelectric response d_{33max}^{t*} in the material is in different directions at different temperatures – at 20°C it is rotated away from the polar axis for an angle of 49.5°, while at temperatures above 65°C, the maximum longitudinal piezoelectric response is along the polar (spontaneous polarization) axis (the off-axis/along-axis threshold for the spontaneous polarization direction change in tetragonal barium titanate is around 62°C, [15]).

In the case of lead titanate (Fig. 2 and Table 2), which is also tetragonal and ferroelectric at room temperature, the maximum piezoelectric effect always remains in the direction of the polar axis, i.e., of the spontaneous polarization direction.

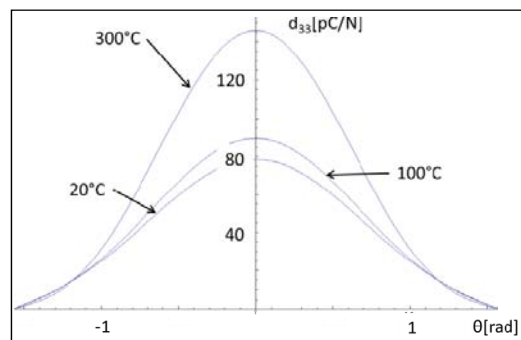


Fig. 2 Angular dependence of the longitudinal piezoelectric coefficient d_{33}^{t*} of tetragonal lead titanate for different temperatures. The angle θ represents the rotation direction away from the tetragonal polar axis. One can see that the maximum piezoelectric response direction in the tetragonal PbTiO₃ single crystal never changes with temperature – it is always along the tetragonal polar axis.

Table 2 Maximum piezoelectric response of the tetragonal lead titanate at selected temperatures – all maxima are along the tetragonal polar axis.

$T(^{\circ}\text{C})$	$d_{33\text{max}}(\text{pC/N})$	$\theta_{\text{max}}(^{\circ})$
20	79	0
100	89	0
300	146	0

From the modelling results presented here, a conclusion can be drawn that the piezoelectric perovskites, that could be used for ultrasonic transducer applications at changing (elevated) temperatures, should not only be considered as materials that are piezoelectric and generally applicable below a certain phase transition temperature and paraelectric above that same temperature, but also that other temperature induced electromechanical effects, such as the presence or the absence of the rotation of the maximal piezoelectric response, should seriously be taken into account while modelling and building probes prototypes. The effect of multiple phase transitions sequences is not exclusively driven by temperature in the perovskite piezoelectrics family; the effect can be caused by external mechanical stress and electric fields.

3. KLM modelling

The piezoelectric response is not the only important material property which changes its anisotropy nature by changing the external thermodynamic conditions (change in temperature, application of external bias electric and mechanical fields, the chemical potential change), but it is the most descriptive one in a piezoelectric material. All other electromechanical properties (such as dielectric constant, mechanical stiffness, density, speed of sound, electromechanical coupling coefficients) change with temperature. These temperature changes and anisotropy can also be straightforwardly calculated in the same manner as it was done for the piezoelectric coefficients in the previous chapter. Changes of all these parameters finally influence significantly the design and functionality of an ultrasound probe, and one has to take them into account. To descriptively show the influence of the temperature influence on the anisotropy, the modelling results from the previous chapter, together with the calculated electromechanical properties, are incorporated directly into the mathematical model of a piezoelectric material based ultrasound NDT transducer. The theoretical tool used is another widely accepted modelling theory based on equivalent electrical circuits, KLM ([22], [23]), with its corresponding commercial software tool, PiezoCAD [24]. Some descriptive modelling results are presented in Fig. 3 - Fig. 6 and Table 3 - Table 6.

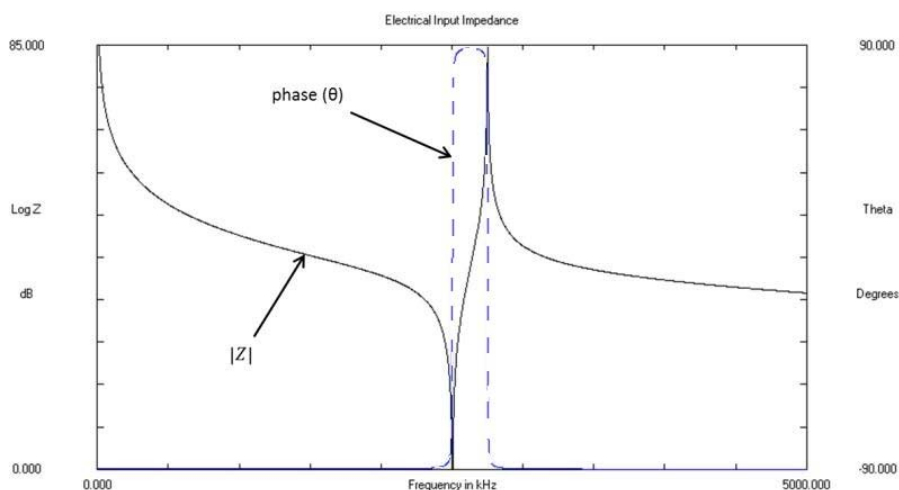
**Fig. 3** Log-lin plot of the frequency dependence of the electrical input impedance amplitude (solid line) and phase angle (dashed line) of a tetragonal barium titanate piezoelectric disc with a diameter of 20 mm and thickness of 1 mm cut perpendicular to the polar axis at room temperature.

Fig. 3 represents the log-lin plot of the frequency dependence of the input electrical impedance (amplitude and phase angle) of a thin disc with a diameter $D = 20$ mm and thickness $t = 1$ mm made of barium titanate at room temperature and cut perpendicular to the polar axis (the vibration direction is parallel to the spontaneous polarization direction). The resonance and the antiresonance frequencies are clearly visible. The central frequency of vibration of the disc is around 2.5 MHz (Table 3). The information about the frequency dependence of the electric input impedance is a key parameter in the electrical impedance matching of the ultrasound probe to the pulse-receive system used to drive the probe.

Table 3 Calculated central frequency and the bandwidth of the piezoelectric barium titanate disc ($D = 20$ mm, $t = 1$ mm) cut perpendicular to the polar axis direction.

Level (dB)	Central frequency (MHz)	Bandwidth (MHz)	Bandwidth (%)
-6	2.548	0.202	7.95
-20	2.545	0.601	23.64
-40	2.529	1.818	71.88

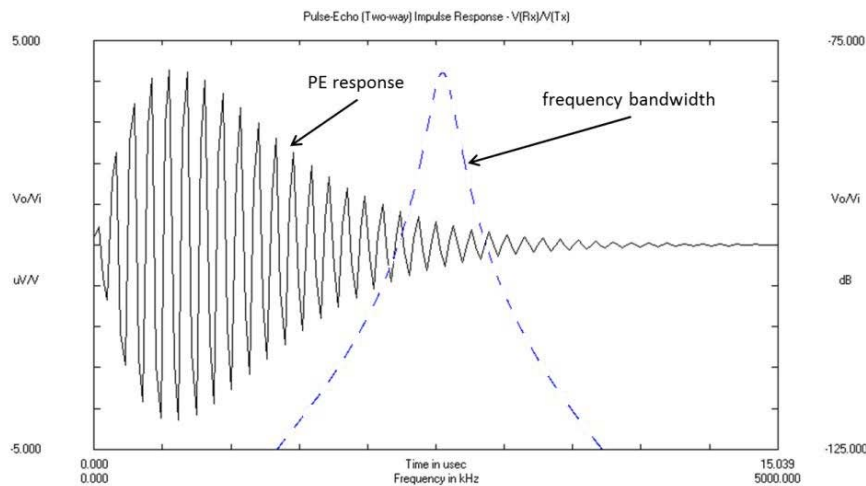


Fig. 4 Time dependence of the pulse-echo impulse response (solid line) and frequency bandwidth (dashed line) of a tetragonal barium titanate piezoelectric disc with a diameter of 20 mm and thickness of 1 mm cut perpendicular to the polar axis at room temperature.

Fig. 4, on the other hand, represents the corresponding time development of the pulse-echo impulse response due to the disc vibration after it was excited by an electrical spike of the normalized voltage ($V_{exc} = 1$ V). The maximal signal response amplitude is around $5 \mu\text{V/V}$, and the disc ringing is significant, which is due to the fact that the disc is freely vibrating in the air.

Table 4 Calculated ultrasound pulse duration of the piezoelectric barium titanate disc ($D = 20$ mm, $t = 1$ mm) cut perpendicular to the polar axis direction at room temperature.

Level (dB)	Pulse width (μs)
-6	3.930
-20	7.824
-40	12.216

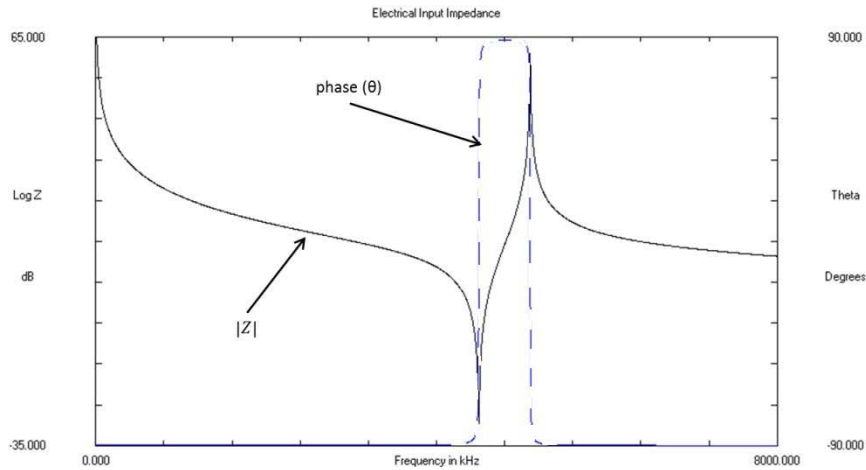


Fig. 5 Log-lin plot of the frequency dependence of the electrical input impedance amplitude (solid line) and phase angle (dashed line) of a tetragonal barium titanate piezoelectric disc with a diameter of 20 mm and thickness of 1 mm cut along the direction $\theta = 49.5^\circ$ away from the polar axis at room temperature.

Fig. 5 shows the log-lin plot of the frequency dependence of the input electrical impedance (amplitude and phase angle) of a thin disc with a diameter $D = 20$ mm, and thickness $t = 1$ mm made of barium titanate at room temperature, but in this case it is cut perpendicular to the direction rotated away from the polar axis for the angle of 49.5° . The resonance and the antiresonance frequencies are clearly visible as in the previously discussed case, but this time the central frequency of vibration of the disc is around 5 MHz (Table 5). The central frequency changed significantly by cutting a barium titanate tetragonal crystal along a direction that is different from the “intuitive” cutting direction perpendicular to the polar axis and the spontaneous dielectric polarization in the material.

Table 5 Calculated central frequency and the bandwidth of the piezoelectric barium titanate disc ($D = 20$ mm, $t = 1$ mm) cut perpendicular to the direction rotated away for 49.5° from the spontaneous polarization direction.

Level (dB)	Central frequency (MHz)	Bandwidth (MHz)	Bandwidth (%)
-6	5.093	0.119	2.35
-20	5.088	0.358	7.05
-40	5.024	1.207	24.03

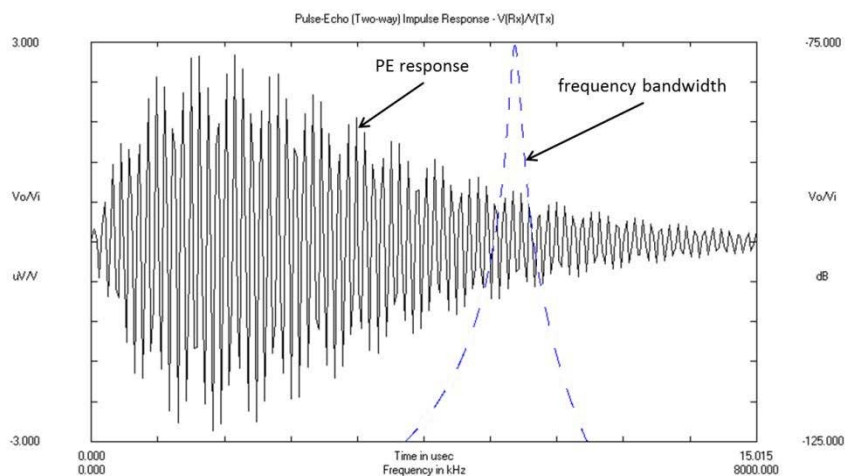


Fig. 6 Time dependence of the pulse-echo impulse response (solid line) and frequency bandwidth (dashed line) of a tetragonal barium titanate piezoelectric disc with a diameter of 20mm and thickness of 1mm cut along the direction $\theta = 49.5^\circ$ away from the polar axis at room temperature.

Correspondingly, Fig. 6 shows the time evolution of the pulse-echo impulse response due to the disc vibration after it was excited by an electrical spike of the normalized voltage ($V_{exc} = 1$ V). The maximal signal response amplitude decreased for around 40% compared to the previous case, and the disc ringing time almost doubled. Thus, different crystal cuts gave different electromechanical responses due to the properties anisotropy.

Table 6 Calculated ultrasound pulse duration of the piezoelectric barium titanate disc ($D = 20$ mm, $t = 1$ mm) cut perpendicular to the direction rotated away for 49.5° from the spontaneous polarization direction.

Level (dB)	Pulse width (μ s)
-6	6.295
-20	12.613
-40	20.200

The modelling results presented in the graphs reflect the fact that the electromechanical material parameters (spontaneous polarization, dielectric, mechanical and piezoelectric constants) change qualitatively with the change in temperature in barium titanate. A detailed explanation of these effects and a generalization to other ferroelectric materials from the same family is given in a series of articles by *M. Budimir et al.*, ([15]-[18]). If one compares the results from the pulse-echo impulse response for barium titanate at 20°C and 65°C (Fig. 4 and Fig. 6), one can see a significant difference in the pulse duration and its maximum amplitude. This shows that both the resolution of transducer based on this material and its radiated output power will be changed significantly with the change in temperature – no same quality of crack resolving in non-destructive evaluation (NDE) can be achieved with the same transducer at these two temperatures, and the main cause is the strong piezoelectric anisotropy.

To discuss the temperature induced changes in the input electrical impedance of the piezoelectric material in question, which is a very important parameter for the transducer design, it is important to mention the relation of the material impedance (Z) to the material constants (its geometrical dimensions l, w, t , the piezoelectric coupling coefficient in the direction of the vibration k_{33} , the frequency of the resonance vibration ω , and the speed of sound in the bulk material at constant applied electric field v_b^E , [40]:

$$\frac{1}{Z} = j\omega \frac{lw}{t} \epsilon_{33}^T \left((1 - k_{33}^2) + k_{33}^2 \frac{\tan(\omega l / 2v_b^E)}{\omega l / 2v_b^E} \right) \quad (7)$$

When the material temperature changes, this will lead to changes in the amplitudes and directions of the electromechanical coefficients, which will lead to changes of the input impedance of the material. This change can be seen in examples presented in Fig. 3 and Fig. 5.

Finally, the modelled barium titanate disc parameters related to the further usage of the barium titanate disc in the NDE ultrasound transducer design have been summarized in the Table 7.

Table 7 A comparison of the barium titanate ultrasound parameters important for the NDE ultrasound testing design at 20°C and 65°C .

Temperature ($^\circ\text{C}$)	Centr. freq. (MHz)	Bandwidth (%)	Signal ampl. ($\mu\text{V}/\text{V}$)	Signal duration (μ s)
20	2.55	7.95	4.67	3.93
65	5.10	2.35	2.93	6.30

4. Conclusion

This paper points out an important issue related to the design and modelling of NDT ultrasound probes planned to be operational at elevated working temperatures. It discusses the effect of the presence or the absence of more than one potential ferroelectric phase in the acoustically active material used in the probe on overall electromechanical and acoustical properties of the probe. The issue is discussed theoretically through the widely used and experimentally verified thermodynamic LGD and equivalent electrical circuit KLM models, using two model materials from the same family of ferroelectric perovskites, from which most of the commercially used acoustically active materials are selected.

The first model material, barium titanate (BaTiO_3), has a temperature induced sequence of ferroelectric-ferroelectric phase transitions, while the other model material, lead titanate (PbTiO_3), has only one possible ferroelectric phase.

The change in the material temperature from room temperature to 100°C or more will induce a continuous rotation of the direction of the maximum piezoelectric response in barium titanate, while the corresponding maximal response direction of lead titanate will remain unchanged at all temperatures. Together with the piezoelectric responses, other electromechanical responses are also anisotropic. This kind of piezoelectric anisotropy is not exclusively related to temperature effects, and this material feature is general for the piezoelectric perovskites family. Thus, when modelling and designing NDT ultrasound probes for elevated temperature applications, one has to take this effect into account to optimize the probe design.

This theoretical work is a part of our wider study of influence of temperature induced piezoelectric anisotropy changes on the design and performance properties of ultrasound NDE transducers. The experimental results will be the subject matter of our future publications.

Acknowledgements

We gratefully acknowledge the financial support of the Unity Through Knowledge Fund, Grant Nr. 47.

REFERENCES

- [1] *4 Die in Accident at Japan Nuclear Power Plant*, article by J. Brooke in New York Times web edition, August 10, 2004, http://www.nytimes.com/learning/teachers/featured_articles/20040810tuesday.html
- [2] *Four dead in Japanese nuclear plant accident*, article in The Sydney Morning Herald web edition, August 10, 2004, <http://www.smh.com.au/articles/2004/08/09/1092022409037.html>
- [3] *Japan nuke plant leakage kills 4 people*, article in the CHINAdaily web edition, August 10, 2004, http://www.chinadaily.com.cn/english/doc/2004-08/10/content_363800.htm
- [4] Long range ultrasonic system for continuous in service inspection and structural health monitoring of high temperature superheated steam pipes in power generation plant with 100% coverage, EC FP7-SME project, 2011, http://cordis.europa.eu/search/index.cfm?fuseaction=proj.document&PJ_RC�=11776340
- [5] Pedrick, M.; Tittmann, B. R.; Seliga, J.: Design and Performance of a Broadband 10 MHz Transducer for Elevated Temperature, Leave-in-Place Applications, *Materials Evaluation*, Vol. 67, No. 2, p.149, 2009.
- [6] Wilcox, P. D.; Lowe, M. J. S.; Cawley, P.: *The excitation and detection of lamb waves with planar coil electromagnetic acoustic transducers*, *IEEE Transactions on ultrasonics, ferroelectrics, and frequency control*, Vol. 52. No. 12, 2005.
- [7] Hernandez-Valle, F.; Dixon, S.: Preliminary tests to design an EMAT with pulsed electromagnet for high temperature, *AIP Conference Proceedings*, 2009., pp. 936-941.
- [8] Idris, A.; Edwards, C.; Palmer, S. B.: *Acoustic Wave Measurements at Elevated Temperature Using a Pulsed Laser Generator and AN Electromagnetic Acoustic Transducer Detector*, *Nondestructive Testing and Evaluation*, Vol. 11, Issue 4, 1994, pp. 195-213.

- [9] Baillie, I., et al.: *Implementing an ultrasonic inspection system to find surface and internal defects in hot, moving steel using EMATs*, Insight., Vol. 49, No. 2, 2007, pp. 87-92.
- [10] Hernandez - Valle, F.; Dixon, S.: *Pulsed electromagnet EMAT for high temperatures*, Rev. Prog. in QNDE 2009. 2010, Vol. 29A&29B, pp. 957-963.
- [11] Kazys, R.; Voleisis, A.; Voleisiene, B.: *High temperature ultrasonic transducers: review*, Ultragasars (Ultrasound), Vol. 63, No. 2, 2008, p.7.
- [12] Turner, R. C.; et al. *Materials for High Temperature Acoustic and Vibration Sensors: A Review*, Applied Acoustics, Vol. 41, 1994, p. 299.
- [13] Damjanovic, D.: *Materials for high temperature piezoelectric transducers*, Current Opinion in Solid State & Materials Science, Vol. 3, 1998, pp. 469-473.
- [14] McNab, A.; Kirk, K. J.; Cochran, A.: *Ultrasonic transducers for high temperature applications*, IEE Proceedings - Science, Measurement and Technology, Vol. 145, 1998, pp. 229-236.
- [15] Budimir, M.; Damjanovic, D.; Setter, N.: *Piezoelectric anisotropy–phase transition relations in perovskite single crystals*, J. Appl. Phys., Vol. 95, No. 10, p. 6753, 2003.
- [16] Budimir, M.; Damjanovic, D.; Setter, N.: *Large enhancement of the piezoelectric response in perovskite crystals by electric bias field antiparallel to polarization*, Appl. Phys. Lett., Vol. 85, No. 14, p.2890, 2004.
- [17] Budimir, M.; Damjanovic, D.; Setter, N.: *Enhancement of the piezoelectric response of tetragonal perovskite single crystals by uniaxial stress applied along the polar axis: A free-energy approach*, Phys. Rev. B 72, 064107, 2005.
- [18] Budimir, M.; Damjanovic, D.; Setter, N.: *Piezoelectric response and free-energy instability in the perovskite crystals BaTiO₃, PbTiO₃, and Pb(Zr,Ti)O₃*, Phys. Rev. B 73, 174106, 2006.
- [19] Landau, L. D: “*Collected papers*”, Oxford: Pergamon Press, p. 546, 1965.
- [20] Devonshire, A. F.: *XCVI. Theory of barium titanate - Part I*, Philosophical Magazine Series 7. Vol. 40, Issue 309, 1949, p.1040-1063.
- [21] Devonshire, A. F.: *CIX. Theory of barium titanate - Part II*, Philosophical Magazine Series 7. Vol. 42, Issue 333, 1951, p.1065-1079.
- [22] Willatzen, M.: *Ultrasound transducer modelling- General Theory and applications to ultrasound reciprocal systems*, IEEE Transactions on Ferroelectrics and frequency control, 2001.
- [23] Lopez-Sanchez, A. L.; Schmerr, L. W.: *A simplified method for complete characterization of an ultrasonic NDE measurement system*, Res. Nondestr. Eval. Springer Verlag Inc, Vol 18, 2006.
- [24] PiezoCAD, Release 3.04, Sonic Concepts, Woodinville, Washington, SAD.
- [25] Mitsui, T.; Tatsuzaki, I.; Nakamura, E.: *An Introduction to the Physics of Ferroelectrics*, Gordon and Breach, London, 1976.
- [26] Jaffe, B.; Cook, W.R.; Jaffe, H.: *Piezoelectric Ceramics*, Academic, New York, 1971.
- [27] Lines, M.E.; Glass, A.M.: *Principles and Applications of Ferroelectric and Related Materials*, Clarendon Press, Oxford, 2001.
- [28] Budimir, M.: *Piezoelectric Anisotropy and Free Energy Instability in Classic Perovskites*, PhD thesis, Ecole Polytechnique Federale de Lausanne, Switzerland, 2006.
- [29] Cox, D. E.; Noheda, B.; Shirane, G; Uesu, Y.; Fujishiro, K.; Yamada, Y.: *Universal phase diagram for high-piezoelectric perovskite systems*, Applied Physics Letter, Vol. 79, 400, Issue 3, 2001
- [30] La-Orauttapong, D.; Noheda, B; YE, Gehring, P. M.; Toulouse, J.; Cox, D. E.; Shirane, G.: *Phase diagram of relaxor ferroelectric (1-x)Pb(Zn_{1/3}Nb_{2/3})O₃-xPbTiO₃*, Physical Review B65, 144101, 2002
- [31] Noheda, B.: *Structure and high-piezoelectricity in lead oxide solid solutions*, Current Opinion in Solid State and Materials Science, Vol. 6, Issue 1, 2002, pg. 27-34.
- [32] Haun, M. J.; Furman, E.; Jang, S. J.; Mc Kinstry H. A.; Cross, L. E., *Thermodynamic theory of PbTiO₃*, J. Appl. Phys. 62, 3331, 1987.
- [33] Kobayshi, J.; Uesu, Y.; Sakemi Y., *X-ray and optical studies on phase transition of PbTiO₃ at low temperatures*, Phys. Rev. B 28, pp. 3866-3872, 1983.
- [34] Landau, L.D.; Lifshitz, E.M.: *Statistical Physics (Volume 5 of A Course of Theoretical Physics)*, Pergamon Press, 1969.
- [35] Bell, A. J., *Phenomenologically derived electric field-temperature phase diagrams and piezoelectric coefficients for single crystal barium titanate under fields along different axes*, J. Appl. Phys. 89, 3907, 2001.

- [36] Goldstein, H.: *Classical Mechanics*, Addison–Wesley, Reading, MA, 1978.
- [37] Nye, J. F.: *Physical Properties of Crystals*, Oxford University, Oxford, 1985.
- [38] Damjanovic, D.; Brem, F.; Setter, N.: *Crystal orientation dependence of the piezoelectric $d(33)$ coefficient in tetragonal BaTiO₃ as a function of temperature*, Appl. Phys. Lett. 80, p. 652-654, 2002.
- [39] Haun, M. J.; Furman, E.; Jang, S. J.; Cross, L. E.: *Thermodynamic theory of the lead zirconate-titanate solid solution system, part I: Phenomenology*, Ferroelectrics Vol. 99, Issue 1, pp. 13-25, 1989.
- [40] Damjanovic, D.: *An Equivalent Electric Circuit of a Piezoelectric Bar Resonator with a Large Piezoelectric Phase Angle*, Ferroelectrics, Vol. 110, pp. 129-135, 1990.

Submitted: 27.6.2012

Accepted: 15.11.2012

Nikola Pavlović, dipl. ing.
Neven Parat, dipl. ing.
Dr. sc. Igor Vuković, dipl. ing.
corresponding author
igor.vukovic@inetec.hr
INETEC – Institute for Nuclear
Technology
Dolenica 28, HR-10250 Zagreb, Croatia